Nuclear Engineering and Technology 55 (2023) 4659–4663

Contents lists available at ScienceDirect

Nuclear Engineering and Technology

journal homepage: www.elsevier.com/locate/net

Original Article

Korean-specific iodine S values for use in internal dosimetry

Tae-Eun Kwon [a,*], Yoonsun Chung [b], Choonsik Lee [a]

[a] Division of Cancer Epidemiology and Genetics, National Cancer Institute, National Institutes of Health, Rockville, MD, 20850, USA
[b] Department of Nuclear Engineering, Hanyang University, Seoul, 04763, South Korea

ARTICLE INFO

Keywords:
Thyroid dose
Internal exposure
Korean phantoms
Specific Absorbed Fraction

ABSTRACT

The use of iodine S values derived using the International Commission Radiological Protection (ICRP) phantoms may introduce significant bias in internal dosimetry for Koreans due to anatomical variability. In the current study, we produced an extensive dataset of Korean S values for selected five iodine radioisotopes (I-125, I-129, I-131, I-133, and I-134) for use in radiation protection. To calculate S values, we implemented Monte Carlo simulations using the Mesh-type Reference Korean Phantoms (MRKPs), developed in a high-quality/fidelity mesh format. Noticeable differences were observed in S value comparisons between the Korean and ICRP reference phantoms with ratios (Korean/ICRP) widely ranging from 0.16 to 6.2. The majority of S value ratios were lower than the unity in Korean phantoms (interquartile range = 0.47-1.28; mean = 0.96; median = 0.69). The S values provided in the current study will be extensively utilized in iodine internal dosimetry for Koreans.

1. Introduction

Internal exposure to radioiodine is one of the general radiation safety concerns. In nuclear accidents, a large amount of radioiodine can be released to environments, causing substantial internal exposure to workers and the public [1,2]. In addition, radioiodine (RAI) therapy, despite its therapeutic intent, can induce substantial radiation exposure to normal tissues beyond the thyroid [3], potentially increasing the risks of radiation-induced adverse effects. To assess these health risks associated with radioiodine intake, it is required to estimate the absorbed doses delivered to each organ and tissue.

For use in internal dosimetry for iodine, the International Commission Radiological Protection (ICRP) has provided the reference dose coefficients (i.e. dose per unit intake, Gy/Bq) [4,5], which were computed using iodine S values (i.e. absorbed doses delivered to target regions per unit disintegration of iodine in source regions, Gy/Bq•s) derived from the ICRP reference computational human phantoms [6]. However, since the ICRP phantoms were established primarily based on Caucasian data [7], applying the ICRP S values to Koreans can introduce significant bias in internal dosimetry due to anatomical differences. To achieve more accurate dose estimation of Koreans, it should be first conducted to calculate iodine S values using Korean computational phantoms.

During the last few decades, multiple Korean computational phantoms have been developed for use in radiation protection, escalating from the first Korean adult male and female voxel phantoms, called Korean Man (KORMAN) and Korean Woman (KORWOMAN) [8], to a series of more elaborate and advanced voxel phantoms based on high-resolution anatomical images, such as Korean Typical Man 1 (KTMAN1), Korean Typical Man 2 (KTMAN2) [8], High-Definition Reference Korean man (HDRK Man) [9] and High-Definition Reference Korean woman (HDRK Woman) [10]. Most recently, a pair of new Korean reference phantoms in a high-quality/fidelity mesh format, called mesh-type reference Korean phantoms (MRKPs) [11], were developed based on new Korean reference anatomical data [12]. However, despite the continuous attempts for the development of Korean computation phantoms, little attention was paid to calculating iodine S values for Koreans. Although Yeom et al. [13] has recently published S values derived from MRKPs, the S value calculation was solely restricted to the thyroid source region and I-131.

To fill this critical research gap, in the current study, we produced an extensive dataset of iodine S values that could be utilized in internal dosimetry for Koreans. To compute iodine S values for Koreans, we implemented Monte Carlo simulations using the MRKPs. The S value calculations were performed for all source regions defined in the latest ICRP biokinetic model for iodine [5]. Since S value calculations would require extensive computation time, in the current study, we selected five iodine radioisotopes for the S value calculations considering their

* Corresponding author. Radiation Epidemiology Branch, Division of Cancer Epidemiology Genetics, National Cancer Institute, NIH, DHHS, 9806 Medical Center Dr, Rockville, MD, 20850, USA.
E-mail address: taeeun.kwon@nih.gov (T.-E. Kwon).

https://doi.org/10.1016/j.net.2023.09.005
Received 10 August 2023; Accepted 4 September 2023
Available online 22 September 2023

importance in radiation protection: I-125, I-129, I-131, I-133, and I-134.

2. Material and methods

2.1. Mesh-type Reference Korean Phantoms (MRKPs)

To overcome the limitations of the voxel-type phantoms on representing thin and/or small organs/tissues arising from the nature of voxel geometry and finite voxel resolutions, the MRKPs were developed in a high-quality/fidelity mesh format using methodology similar to that employed in the development of new ICRP Mesh-type Reference Computational Phantoms (MRCPs) [14]. The MRKPs include all source and target regions needed for calculating effective dose, even the micrometer-thick source and target regions in the respiratory and alimentary tract organs, skin, and urinary bladder. Thus, the MRKPs facilitate more realistic dose evaluation for very thin target regions such as urinary bladder walls of 118–193 μm and 116–185 μm for adult male and female, respectively. Moreover, the MRKPs were constructed based on a new set of Korean reference anatomical data reflecting body size and shape of the present age [12]. The new Korean anatomical data includes masses for 58 organs/tissues, which were derived by collecting and analyzing data from various literature. In particular, the reference masses of thyroid (15 g and 12 g for male and female, respectively), the most important organ in terms of iodine internal exposure, were taken from those derived by actual measurements on healthy volunteers (66 males and 55 females) [15]. Based on the new Korean reference anatomical data, anthropometric dimensions of the MRKPs were all adjusted. Details on the MRKPs and the Korean anatomical data can be found elsewhere [11].

2.2. S value calculation

To calculate iodine S values for Koreans, we implemented the MRKPs in the PHITS (Particle and Heavy Ion Transport code System) Monte Carlo code [16]. Within the PHITS framework, we designated the source type in [Source] as 's-type = 24' to generate particles from tetrahedron geometry and specified source regions using the 'tetreg' option with an assumption of iodine homogeneously distributed in the source regions. For source regions distributed throughout the body, we used the multi-source option (i.e., <source>), allowing for assignment of relative weights to each source region; for example, for the blood source region, particles emitted from each cell containing blood fractions were weighted by the corresponding blood volumes of each cell and then normalized against the total blood volume. To maximize computational efficiency, we directly calculated S values without considering specific absorbed fractions (SAFs). Thus, beta and gamma particles were competitively generated in each calculation according to iodine decay schemes (i.e. energy and emission yield).

We performed S value calculations for total 26 source regions, defined in the latest ICRP reference iodine biokinetic model [5], the revised human respiratory tract model (the revised HRTM) [17], and the human alimentary tract model (HATM) [18], and for 30 radiosensitive target regions associated with effective dose (Table 1). In respiratory tract regions of the MRKPs (i.e. bronchial (BB), bronchiolar (bb), and alveolar-interstitial (AI) regions), airway generations 2–8 of BB region and all generations of bb region (i.e. airway generation 9–15) were developed in the constructive solid geometry (CSG) format, which could not be utilized in the PHITS code. In response to this challenge, we employed the following methodologies to calculate S values for respiratory tract regions. For electron S values for BB, bb, AI source regions, we performed a scaling of the S values provided in ICRP Publication 133 [6] using the differences in target masses between the Korean and ICRP reference phantoms. For photon S values for bb and AI source and target regions, we used the entire lungs as a surrogate tissue. Note that photon S values for BB regions, constructed only with initial generations of airway branching, can be directly calculated.

Table 1
Source and target region list for S value calculations.

Source region[a]	Target region[a]
Alveolar-interstitium	Red bone marrow
Total blood	Colon
Bronchiolar	Lungs
Bronchiolar sequestered region	Stomach
Bronchial	Breasts
Bronchi sequestered region	Ovaries
ET_1 surface	Testes
ET_2 sequestered region	Urinary bladder
ET_2 surface	Oesophagus
Kidneys	Liver
Left colon contents	Thyroid
ET lymph nodes	Endosteum
Thoracic lymph nodes	Brain
Liver	Salivary glands
Oral cavity	Skin
Oesophagus fast	Adrenal
Oesophagus slow	ET of HRTM
Other tissue	Gallbladder
Right colon contents	Heart
Rectosigmoid colon contents	Kidneys
Salivary glands	Lymph nodes
Small intestine contents	Muscle
Stomach contents	Oral mucosa
Stomach wall	Pancreas
Thyroid	Prostate
Urinary bladder content	Uterus
	Small intestine
	Spleen
	Thymus
	Eye lens

[a] ET_1: anterior nasal passage; ET_2: posterior nasal passage, pharynx, and larynx; ET: extrathoracic; HRTM: human respiratory tract model.

Absorbed doses for target regions were directly tallied by [T-deposit] except for skeletal tissues, not explicitly represented within the tetrahedral structure of the MRKPs. For skeletal tissues (i.e., RBM and endosteum), S values were derived from the absorbed doses to the spongiosa and medullary marrow, in line with the approach outlined in ICRP Publication 116 [19]. For electrons, absorbed doses for skeletal tissues were approximated as a mass-weighted average of the doses to the regional spongiosa and medullary cavity. For photons, we employed an approach based on fluence-to-absorbed dose response functions. The energy-dependent fluences to skeletal tissues were calculated using [T-tract] tally and then converted to skeletal absorbed doses by applying the fluence-to-absorbed dose response functions (DRFs) derived from MRKPs. 10^9 particles were generated for each calculation with cut-off energy of 1 keV. The simulations were performed by a high-performance computing cluster of Innovative Technology Center for Radiation Safety (iTRS).

We compared the S values ($r_T \leftarrow$thyroid) for I-131 computed in our study with those determined by Yeom et al. The latter employed the same human phantoms (MRKPs) but used a different computational code (Geant 4) and a larger number of particles (10^{10}). The self-absorption S values for thyroid (thyroid←thyroid) were also compared with mass-scaled S values, derived by scaling S values from ICRP Publication 133 [6] according to the differences in thyroid masses between the Korean phantoms (15 g and 12 g for adult male and female, respectively) and the ICRP reference voxel phantoms (23.4 g and 19.5 g for adult male and female, respectively). To quantify the dosimetric impact of the Korean S values, we performed S value comparisons between the Korean phantoms and the ICRP reference voxel phantoms [20] across five major source regions (i.e. salivary glands, stomach wall, kidneys, liver, and thyroid), five target regions with a tissue weighting factor of 0.12 (i.e. red bone marrow, stomach, colon, lungs, and breasts), and the five iodine isotopes. In particular, the S values ($r_T \leftarrow$thyroid) for I-131 were contrasted more thoroughly with those derived from the ICRP phantoms.

3. Results

3.1. Iodine S values for Koreans

A library of S values for 26 source regions, 30 target regions, and 5 isotopes was created. Full data is available in the electronic appendix. Table 2 shows an example of S value in the case of S(r_T←thyroid) for I-131 compared with those calculated by Yeom et al. [13]. The S values of the current study were comparable to those of Yeom et al. with the ratios ranging from 0.94 to 1.15. The relative errors for most S values were less than 10%. While the S values for testes and prostate showed higher relative errors, exceeding 10%, they still agreed with those calculated by Yeom et al. The mass-scaled thyroid self-absorption S values derived from ICRP reference values were 2.08E-09 and 2.61E-09 for Korean adult males and females, respectively, which were close to those calculated in the current study.

3.2. Comparison of S values with the ICRP reference phantoms

The significant differences were observed in the comparison of S values (r_T←thyroid) for I-131 between the Korean and ICRP reference voxel phantoms (Fig. 1). The ratios of S values (r_T←thyroid) of the Korean phantoms to those of the ICRP phantoms ranged widely from 0.25 to 3.61, and the greatest differences were observed in S value (ET←thyroid) and S value (colon←thyroid) for male and female phantoms, respectively. The majority of S values were lower in the Korean phantoms than in the ICRP reference phantoms although a few were higher in the Korean phantoms. Certain target regions showed opposing trends in the S value comparison between the male and female phantoms; for instance, the S value (colon←thyroid) of the Korean phantom was lower for male (ratio = 0.36) but significantly higher for female (ratio = 2.28) in comparison to those of the ICRP phantoms. Importantly, the thyroid self-absorption S values (thyroid←thyroid) were notably higher in the Korean phantoms with ratios of 1.57 and 1.63 for male and female phantoms, respectively.

Greater differences were observed in the expanded comparisons of S values for the major source-target region pairs and the five isotopes between the Korean and ICRP phantoms (Fig. 2). The S value ratios (Korean/ICRP) widely ranged from 0.16 to 6.2; however, the majority of S values were lower in Korean phantoms (interquartile range = 0.47-1.28, mean = 0.96, median = 0.69). In particular, the S value ratios for male phantoms tend to be lower (interquartile range = 0.43-0.97, mean = 0.75, median = 0.59) than for female phantoms (interquartile range = 0.58-1.6, mean = 1.18, median = 0.78). The greatest ratios were found in S value (breasts←salivary gland) and S value (breasts←stomach wall) for male and female phantoms, respectively.

Table 2
S values (r_T←thyroid) for I-131 [mGy (Bq s)$^{-1}$] based on MRKPs.

Target Organs[a]	Adult male		Adult female	
	S value (Relative error)	Ratio[b]	S value (Relative error)	Ratio[b]
R-marrow	3.46E-13 (8.6E-06)	0.94	4.07E-13 (9.5.E-06)	0.95
Colon	1.08E-14 (7.7E-03)	1.00	2.23E-14 (7.0.E-03)	0.95
Lungs	4.55E-13 (9.1E-04)	1.00	5.25E-13 (9.8.E-04)	1.00
St-wall	4.02E-14 (6.3E-03)	1.02	6.97E-14 (4.4.E-03)	0.97
Breast	1.38E-13 (1.2E-02)	1.03	1.34E-13 (3.8.E-03)	0.99
Testes	5.19E-16 (1.6E-01)	1.07	3.33E-15 (7.7.E-02)	0.93
UB-wall	1.75E-15 (4.9E-02)	1.02	2.20E-15 (6.9.E-02)	0.95
Oesophagus	3.93E-12 (2.5E-03)	1.13	4.32E-12 (1.9.E-03)	1.00
Liver	8.46E-14 (1.2E-03)	0.99	1.47E-13 (1.8.E-03)	0.99
Thyroid[c]	2.10E-09 (1.0E-04)	0.96	2.61E-09 (9.7.E-05)	0.96
Endosteum	2.63E-13 (9.4E-06)	0.95	3.11E-13 (9.8.E-06)	0.96
Brain	1.32E-13 (1.1E-03)	0.99	2.42E-13 (1.3.E-03)	0.99
S-glands	8.25E-13 (2.4E-03)	1.00	1.40E-12 (2.2.E-03)	0.99
Skin	1.60E-13 (8.5E-04)	1.07	2.10E-13 (7.5.E-04)	1.06
Adrenals	4.61E-14 (1.9E-02)	0.90	9.69E-14 (1.6.E-02)	1.01
ET	7.47E-12 (8.0E-04)	1.05	4.01E-12 (1.5.E-03)	0.96
GB-wall	3.15E-14 (4.9E-02)	1.04	1.05E-13 (2.4.E-02)	1.03
Ht-wall	3.71E-13 (1.3E-03)	0.99	5.16E-13 (2.0.E-03)	0.99
Kidneys	2.58E-14 (5.5E-03)	0.99	5.70E-14 (3.5.E-03)	0.99
LN	2.61E-13 (3.0E-03)	0.99	3.19E-13 (2.7.E-03)	0.99
Muscle	2.33E-13 (2.0E-04)	0.99	3.07E-13 (3.8.E-04)	0.99
O-mucosa	8.00E-13 (2.1E-02)	1.00	1.58E-12 (2.1.E-02)	0.99
Pancreas	3.23E-14 (1.2E-02)	0.94	5.94E-14 (7.9.E-03)	0.99
Prostate	1.07E-15 (1.1E-01)	1.15	1.54E-14 (6.0.E-03)	1.00
SI-wall	8.49E-15 (7.8E-03)	1.09	8.37E-14 (5.0.E-03)	0.99
Spleen	3.77E-14 (3.3E-03)	0.97	2.20E-12 (1.8.E-03)	0.99
Thymus	2.27E-12 (2.5E-03)	0.99	3.14E-15 (1.9.E-02)	1.05

[a] R-marrow: red bone marrow; St-wall: stomach wall; UB-wall: urinary bladder wall; S-glands: salivary glands; ET: extrathoracic region; GB-wall: gall-bladder wall; Ht-wall: heart wall; LN: lymph nodes; O-mucosa: oral mucosa; SI-wall: small intestine wall.

[b] The ratio of S values in the current study to those calculated by Yeom et al. [13].

[c] Mass-scaled thyroid self-absorption S values: 2.08E-09 and 2.61E-09 mGy (Bq s)$^{-1}$ for adult male and female, respectively.

4. Discussion

The current study was aimed to provide a dataset of iodine S values specific for Koreans for use in internal dosimetry. Our findings show that there are significant differences in S values between the Korean and ICRP reference phantoms, stressing the need for Korean-specific S values. To our knowledge, this is the first attempt to compute S values using the Korean reference phantoms covering all source and target regions required for iodine internal dosimetry.

A good agreement observed in the comparison of S values (r_T←thyroid) for I-131 between the current study and the work of Yeom et al. [13] mutually supports the reliability of the findings of both studies. Despite fewer particles being transported in the current study, the calculated S values were overall comparable in both studies. It is plausible that the small differences in the S values between the two studies arose from the difference in the Monte Carlo codes used. Although a 15% difference was observed in the S value (prostate←thyroid) for male phantoms, the absolute difference may not be of great importance in terms of dose assessment because the S value (prostate←thyroid) is remarkably lower by a factor of 10^5 than the S value (thyroid←thyroid), which may be the most substantial contributor to thyroid absorbed doses. The self-absorption S values (thyroid←thyroid) in the current study were also consistent with the thyroid mass-scaled S values, which were simply scaled from the ICRP reference S values. This result demonstrates not only the reliability of our results but also the feasibility of the mass-scaling method for thyroid dose, frequently employed in nuclear medicine to account for patient-specific thyroid mass.

We also compared the S values (r_T←thyroid) for I-131 in the current study with those derived from the ICRP reference phantoms to investigate the dosimetric impact arising from employing the Korean phantoms. Interestingly, even with the relatively small differences in body height and weight between Korean and ICRP phantoms (172 cm/74 kg vs. 176 cm/73 kg for male phantoms and 159 cm/57 kg vs. 163 cm/60 kg for female phantoms), the differences in S values turned out to be remarkably significant. In particular, it is noteworthy that the Korean phantoms, whose body height and weight are comparable to, or even less than, those of the ICRP phantoms, exhibited predominantly lower S values.

S values, by definition, can be affected by a fraction of energy of radiation emitted within the source region that is absorbed in the target region (referred to as Absorbed Fraction, or AF) and/or the target region mass. Since self-absorption AFs for beta particles, which predominantly contribute to self-irradiation, can generally be assumed to be 1 and are scarcely affected by organ geometry, the differences in the self-absorption S values (thyroid←thyroid) between the two types of phantoms can be explained by the differences in the target region masses. Note that the ratios of the S values (thyroid←thyroid) of the Korean phantoms to those of the ICRP phantoms (e.g. 1.57 for male phantoms)

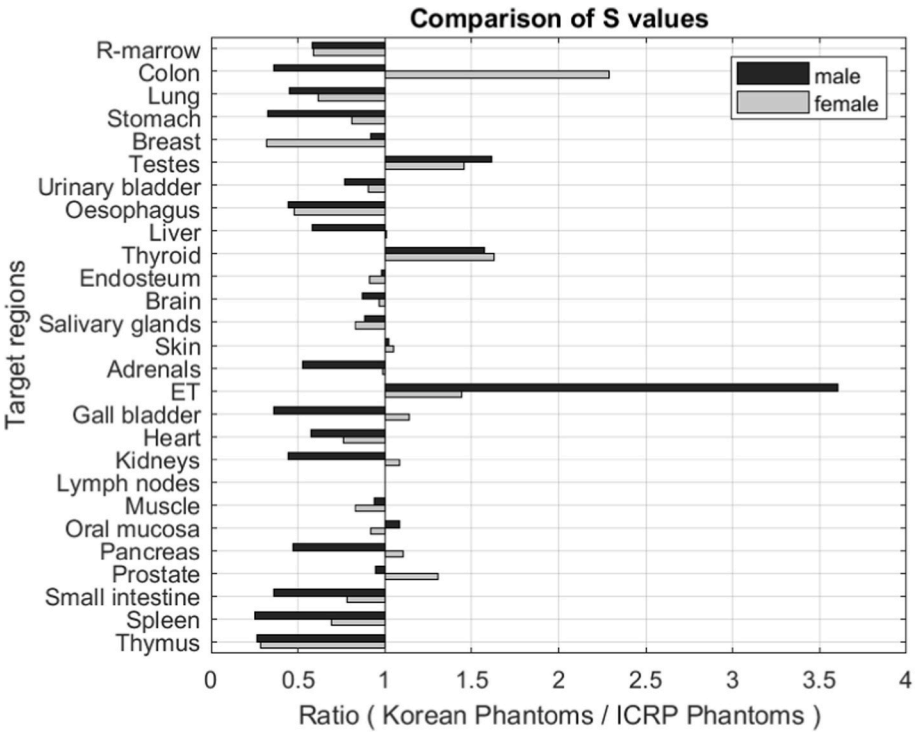

Fig. 1. Ratios of S values ($r_T \leftarrow$thyroid) for I-131 calculated in the current study to those from the ICRP reference voxel phantoms [6].

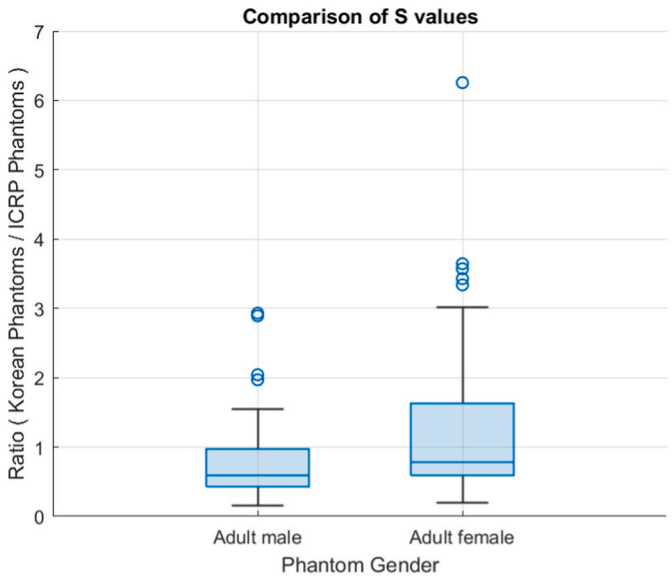

Fig. 2. Ratios of S values (Korean/ICRP) for major source-target region pairs (source regions: salivary glands, stomach wall, kidneys, liver, and thyroid; target regions: red bone marrow, stomach, colon, lungs, and breasts) and the selected five iodine isotopes (I-125, I-129, I-131, I-133, and I-134). (For interpretation of the references to color in this figure legend, the reader is referred to the Web version of this article.)

were consistent with the inverse of the thyroid mass ratios (e.g. 1/(15 g/23.4 g) = 1.56 for male phantoms). On the contrary, the crossfire S values (i.e. S values with different source and target regions) are mainly determined by photon AFs, which are heavily affected by distances between source and target regions. As the distance between source and target regions increases, average flight lengths of photons become longer, causing a decrease of intensity of photons directed toward target regions. Therefore, the large differences in the crossfire S values can be explained by the differences in the source-to-target region distances between the Korean and ICRP phantoms. In other words, the S values observed in the Korean phantoms indicate that the distances from the thyroid to target regions may be longer in the Korean phantoms. This analysis was also addressed in the study of Yeom et al. [13]. They performed a direct comparison of the chord length distributions (CLDs) from the thyroid to the target regions between the Korean phantoms and the ICRP mesh-type reference computational phantoms [14]. Their findings revealed that the Korean phantoms generally exhibited longer CLDs for most target regions.

The differences in the S values between the Korean and ICRP phantoms, resulting from the differences in the source-to-target region distances, were more substantially revealed in the S value comparison performed across the major source-to-target region pairs, which may greatly contribute to effective dose. In particular, for the male phantoms, the majority of S values in the Korean phantoms were lower than those in the ICRP phantoms (the interquartile range of the ratio (Korean/ICRP) = 0.43-0.97), and the differences against the ICRP phantoms were greater compared to the female phantoms (the median of the ratio = 0.59 vs. 0.78 for male and female phantoms, respectively). Therefore, the differences in the source-to-target region distances between the Korean and ICRP phantoms are presumed to be larger in the male phantoms than in the female phantoms.

As previously discussed, a source-to-target region distance is one of the most influential factors in S value calculations. However, it is necessary to further discuss the fact that the Korean phantoms with relatively smaller body sizes tend to have the longer source-to-target region distances than the ICRP phantoms, thus resulting in the general trend of the lower S values. Although reference computational human phantoms should be able to ideally represent anatomical/morphological characteristics of the population of interest, no reference data on organ or tissue locations that can be used for phantom developments are available. Thus, computational human phantoms are generally constructed from anatomical images obtained from a particular individual with the reference height and weight, without accounting for distances between organs or tissues. In light of these, there is a potential that the differences in the source-to-target region distances between the Korean

and ICRP phantoms arose not from the inter-population variability (i.e. the anatomical differences between Koreans and ICRP reference person) but from the inter-individual variability caused by the use of images from a single individual. For more evidence-based discussions, it is necessary to further investigate representativeness of organ/tissue locations in computational phantoms.

We are aware of the following limitations of the current study. First, the Korean phantoms, developed based on the Korean reference anatomy data, may not fully explain the anatomy of a specific individual. Thus, the S values in the current study may not be applicable to individuals with non-reference body height and weight due to the inter-individual anatomical variability. In particular, variations in organ/tissue locations (i.e. source-to-target region distances) could introduce substantial uncertainty in S values. To achieve a more precise dose estimation for individuals, individual-specific anatomy should be considered. Second, due to a technical issue in the simulation code we used, S values for several respiratory tract regions in the Korean phantoms were not directly calculated but derived by scaling the ICRP reference values. To enhance the accuracy of dose estimation for these respiratory tract regions, direct calculations of S values using the Korean phantoms are necessary. Lastly, while we partially validated our results through the comparisons with other data, some of the S values we calculated still have high relative errors due to the limited number of particles. To obtain more refined S values, additional simulations with a greater number of particles should be performed, even if substantial differences are not anticipated.

5. Conclusion

We created a comprehensive dataset of Korean S values for 28 source regions and 30 target regions, focusing on five selected iodine isotopes. To compute these S values, we implemented Monte Carlo simulations using the adult Korean reference phantoms, which were constructed in a high-quality/fidelity mesh format. We noted considerable differences in the S values between the Korean and ICRP reference phantoms, primarily attributable to anatomical variability. The S values presented in the current study would allow for Korean-specific internal dosimetry for iodine and be widely utilized in a range of fields, including nuclear emergency management, nuclear medicine, and radiation safety regulation.

Declaration of competing interest

The authors declare that they have no known competing financial interests or personal relationships that could have appeared to influence the work reported in this paper.

Acknowledgments

This research was funded by the intramural research program of the National Institutes of Health (NIH), National Cancer Institute, Division of Cancer Epidemiology and Genetics.

Appendix A. Supplementary data

Supplementary data to this article can be found online at https://doi.org/10.1016/j.net.2023.09.005.

References

[1] E. Kim, K. Yajima, S. Hashimoto, K. Tani, Y. Igarashi, T. Iimoto, N. Ishigure, H. Tatsuzaki, M. Akashi, O. Kurihara, Reassessment of internal thyroid doses to 1,080 children examined in a screening survey after the 2011, Fukushima Nucl. Disaster Health Phys. 118 (2020) 36–52.
[2] V. Drozdovitch, V. Minenko, V. Khrouch, S. Leshcheva, Y. Gavrilin, A. Khrutchinsky, T. Kukhta, S. Kutsen, N. Luckyanov, S. Shinkarev, S. Tretyakevich, S. Trofimik, P. Voilleque, A. Bouville, Thyroid Dose Estimates for a Cohort of Belarusian Children Exposed to Radiation from the Chernobyl Accident Radiation Research, vol. 179, 2013, pp. 597–609.
[3] T.-E. Kwon, E. Pasqual, C.M. Kitahara, C. Lee, Absorbed dose coefficients for adult thyroid cancer patients undergoing radioiodine therapy, J. Radiol. Prot. 43 (2023), 021510.
[4] ICRP, Age-dependent doses to members of the public from intake of radionuclides: Part 5. Compilation of ingestion and inhalation dose coefficients, Ann. ICRP 26 (1996) 1–91.
[5] ICRP, Radiation dose to patients from radiopharmaceuticals: a compendium of current information related to frequently used substances, Ann. ICRP (2015) 44 7–321.
[6] ICRP, The ICRP computational framework for internal dose assessment for reference adults: specific absorbed fractions, Ann. ICRP 45 (2016) 1–74.
[7] ICRP, Basic anatomical and physiological data for use in radiological protection : reference values ICRP publication 89, Ann. ICRP (2002) 32 1–277.
[8] C. Lee, S. Park, J.K. Lee, Development of the two Korean adult tomographic models, Med. Phys. 33 (2006) 380–390.
[9] C.H. Kim, S.H. Choi, J.H. Jeong, C. Lee, M.S. Chung, HDRK-man: A Whole-Body Voxel Model Based on High-Resolution Color Slice Images of a Korean Adult Male Cadaver Physics in Medicine and Biology, vol. 53, 2008, pp. 4093–4106.
[10] Y.S. Yeom, J.H. Jeong, C.H. Kim, M.C. Han, B.K. Ham, K.W. Cho, S.B. Hwang, HDRK-Woman: whole-body voxel model based on high-resolution color slice images of Korean adult female cadaver, Phys. Med. Biol. 59 (2014) 3969–3984.
[11] C. Choi, T.T. Nguyen, Y.S. Yeom, H. Lee, H. Han, B. Shin, X. Zhang, C.H. Kim, B. S. Chung, Mesh-type reference Korean phantoms (MRKPs) for adult male and female for use in radiation protection dosimetry, Phys. Med. Biol. 64 (2019), 085020.
[12] C. Choi, Y.S. Yeom, T.T. Nguyen, H. Lee, H. Han, B. Shin, X. Zhang, C.H. Kim, B. S. Chung, Korean anatomical reference data for adults for use in radiological protection, J. Korean Phys. Soc. 72 (2018) 183–191.
[13] Y.S. Yeom, B. Shin, C. Choi, H. Han, C.H. Kim, Iodine-131 S values for use in organ dose estimation of Korean patients in radioiodine therapy, Nucl. Eng. Technol. 54 (2022) 689–700.
[14] ICRP, Adult mesh-type reference computational phantoms, Ann. ICRP 49 (2020) 13–201.
[15] S. Park, J.K. Lee, J.I. Kim, Y.J. Lee, Y.K. Lim, C.S. Kim, C. Lee, In vivo organ mass of Korean adults obtained from whole-body magnetic resonance data, Radiat. Prot. Dosim. 118 (2006) 275–279.
[16] T. Sato, Y. Iwamoto, S. Hashimoto, T. Ogawa, T. Furuta, S. Abe, T. Kai, P.-E. Tsai, N. Matsuda, H. Iwase, N. Shigyo, L. Sihver, K. Niita, Features of particle and Heavy Ion Transport code System (PHITS) version 3.02, J. Nucl. Sci. Technol. 55 (2018) 684–690.
[17] ICRP, Occupational intakes of radionuclides: Part 1, Ann. ICRP 44 (2015) 5–188.
[18] ICRP, Human alimentary tract model for radiological protection ICRP publication 100, Ann. ICRp 36 (2006) 1–336.
[19] ICRP, Conversion coefficients for radiological protection quantities for external radiation exposures ICRP publication 116, Ann. ICRP 40 (2010) 1–258.
[20] ICRP, Adult reference computational phantoms ICRP publication 110, Ann. ICRP 39 (2009) 1–166.